

Synthesis and characterisation of the hexanuclear ruthenium diphosphine clusters $[\text{Ru}_6\text{C}(\text{CO})_{15}\{\mu\text{-Ph}_2\text{P}(\text{CH}_2)_n\text{PPh}_2\}]$ ($n = 1\text{--}4$); crystal structures where $n = 1\text{--}3$

Trushar Adatia,^a Gráinne Conole,^a Simon R. Drake,^b Brian F. G. Johnson,^b Margalith Kessler,^a Jack Lewis^b and Mary McPartin^a

^a School of Chemistry, University of North London, London N7 8D, UK

^b University Chemical Laboratory, Lensfield Road, Cambridge CB2 1EW, UK

Treatment of a hexane solution of the complex $[\text{Ru}_6\text{C}(\text{CO})_{17}]$ and 1 equivalent of the organodiphosphine ligands $\text{Ph}_2\text{P}(\text{CH}_2)_n\text{PPh}_2$ ($n = 1\text{--}3$) produced the series of derivatives $[\text{Ru}_6\text{C}(\text{CO})_{15}\{\mu\text{-Ph}_2\text{P}(\text{CH}_2)_n\text{PPh}_2\}]$ **1**–**3**, respectively, in ca. 74–94% yield. These clusters have been characterised by IR and NMR spectroscopy and in the solid state by X-ray analyses. The three related compounds all adopt a similar octahedral metal core geometry with the bidentate diphosphine ligand bridging one Ru–Ru edge of the metal polyhedron. Reaction of $[\text{Ru}_6\text{C}(\text{CO})_{17}]$ with 1,4-bis(diphenylphosphine)butane, $\text{Ph}_2\text{P}(\text{CH}_2)_4\text{PPh}_2$, yielded two products which differ in the mode of bonding of the diphosphine ligand, the major product $[\text{Ru}_6\text{C}(\text{CO})_{16}\{\text{Ph}_2\text{P}(\text{CH}_2)_4\text{PPh}_2\text{-}P\}]$ **4a** in ca. 74% yield and the minor product $[\text{Ru}_6\text{C}(\text{CO})_{15}\{\mu\text{-Ph}_2\text{P}(\text{CH}_2)_4\text{PPh}_2\}]$ **4b** in ca. 10% yield.

The chemistry of binuclear metal complexes containing chelating diphosphine ligands is now well established.^{1–3} In recent years bridging phosphine groups have been used in metal cluster chemistry because of their ability to maintain the integrity of the metal core intact during chemical reactions and to act as templates for the synthesis of metal–metal bonds by bridge-assisted reactions.^{4–6} From these studies it has been found that in the solid state the diphosphine groups adopt a variety of bonding modes on the cluster surface including monodentate, chelating, edge-bridging and even an example of the ligand spanning the base of a square pyramid.^{7–10}

It has been well established that direct substitution of carbonyl ligands in $[\text{Ru}_6\text{C}(\text{CO})_{17}]$ by monodentate phosphines is possible under mild conditions^{11,12} but similar studies with diphosphines are still relatively rare.^{11,13} This work reports the results of the reactions of a series of diphosphines $\text{Ph}_2\text{P}(\text{CH}_2)_n\text{PPh}_2$ [dppm ($n = 1$), dppe ($n = 2$), dppp ($n = 3$), dppb ($n = 4$)] with the hexanuclear cluster $[\text{Ru}_6\text{C}(\text{CO})_{17}]$ which produce the cluster series $[\text{Ru}_6\text{C}(\text{CO})_{15}\{\text{Ph}_2\text{P}(\text{CH}_2)_n\text{PPh}_2\}]$ ($n = 1$, **2**, **3** or **4**). Full crystal structure analyses of **1**,* **2** and **3** have been made. These compounds enable a comparison of the structural variations that arise from lengthening the organic backbone in the diphosphine ligand. Reaction of $[\text{Ru}_6\text{C}(\text{CO})_{17}]$ with dppb also gives the compounds $[\text{Ru}_6\text{C}(\text{CO})_{16}\{\text{Ph}_2\text{P}(\text{CH}_2)_4\text{PPh}_2\}]$ **4a** and $[\text{Ru}_6\text{C}(\text{CO})_{15}\{\text{Ph}_2\text{P}(\text{CH}_2)_4\text{PPh}_2\}]$ **4b** for which NMR studies indicate that in the major product (**4a**) the diphosphine ligand adopts an unusual *P*-pendant bonding mode, whilst in the minor product (**4b**) it adopts the more common *P*₂*P'*-edge-bridging configuration.

Results and Discussion

Under reflux in a solution of hexane the hexaruthenium cluster $[\text{Ru}_6\text{C}(\text{CO})_{17}]$ reacts immediately on mixing with the chelating diphosphines $\text{Ph}_2\text{P}(\text{CH}_2)_n\text{PPh}_2$ ($n = 1\text{--}3$) to give the black products **1**–**3** formulated on the basis of their IR, NMR and mass

spectral data (Table 1). For **1** the expected triplet for the PCH_2P group is observed in the room-temperature solution ¹H NMR spectrum and the ³¹P-¹H NMR spectrum at 294 K shows a sharp singlet indicating that the two phosphorus atoms of the dppm ligand are equivalent. On cooling to 190 K two signals are observed for two inequivalent phosphorus atoms (Table 1). The ¹H NMR spectrum for the analogous dppe cluster **2** shows an AA'BB' multiplet centred at δ 2.45 for the methylene groups, which have become more complex due to non-first-order coupling from the phosphorus atoms. The ³¹P-¹H NMR spectrum shows a single broad peak for the two phosphorus atoms of the dppe ligand in the temperature range 188–293 K (Table 1). The ¹H NMR spectrum of the dppp cluster $[\text{Ru}_6\text{C}(\text{CO})_{15}\{\mu\text{-Ph}_2\text{P}(\text{CH}_2)_3\text{PPh}_2\}]$ **3** shows a doublet of triplets at δ 2.70 for the two outer methylene protons and a doublet of triplets of triplets at δ 1.71 for the protons of the central methylene group and no second-order coupling from the phosphorus atom is observed (Table 1). The ³¹P-¹H NMR spectrum shows a broad singlet for the two equivalent phosphorus atoms of the dppp ligand at 293 K, and on cooling to 192 K two signals in an AB pattern are observed. At room temperature each of the three compounds exhibits one broad resonance in the ¹³C NMR spectrum for the carbonyl ligands centred at δ 202.34 for **1**, 202.93 for **2** and 203.42 for **3**. These high-frequency (low-field) signals are commonly observed with phosphine substitution.¹⁴

The reaction of the parent complex $[\text{Ru}_6\text{C}(\text{CO})_{17}]$ with 1,4-bis(diphenylphosphino)butane (dppb) results in the formation of two products, which have been formulated on the basis of IR, NMR and mass spectra as $[\text{Ru}_6\text{C}(\text{CO})_{16}\{\text{Ph}_2\text{P}(\text{CH}_2)_4\text{PPh}_2\text{-}P\}]$ **4a** and $[\text{Ru}_6\text{C}(\text{CO})_{15}\{\mu\text{-Ph}_2\text{P}(\text{CH}_2)_4\text{PPh}_2\}]$ **4b** (Table 1). The ¹H NMR spectrum of **4a** was found to contain several broad multiplets which could not be easily resolved. The ³¹P-¹H NMR spectrum revealed two doublets with one of these resonances comparable to that of the free diphosphine at δ –157.22 (relative to trimethyl phosphite) with the other resonance showing a shift to high field at δ –104.01. The phosphorus–phosphorus coupling, ³J(PP), of 35.9 Hz observed in this spectrum is typical of a monoco-ordinated diphosphine group.⁷ This pendant mode of diphosphine ligands has previously been observed in the pentanuclear cluster $[\text{Os}_5\text{C}(\text{CO})_{15}(\text{dppe})\text{-}P]$.⁷ The minor product **4b** was the only member of the series under investigation that was found to be air sensitive in solution. On

* The crystal structure of compound **1** has previously been reported¹³ but neither spectroscopic nor synthetic details were included. The redetermination using the excellent crystals obtained in this work has yielded better crystallographic parameters, which are employed in comparison with the remaining two members of the series and full synthetic and spectroscopic details are given.

Table 1 Spectroscopic data for compounds **1–4b**

Compound	$\nu_{\max}(\text{CO})^a/\text{cm}^{-1}$	NMR ^b			Mass spectrum ^c <i>m/z</i>
		¹ H	¹³ C	³¹ P- ¹ H	
1	2071s, 2034s, 2019vs, 1979m (sh), 1956w (sh), 1831w (br)	7.3 (m Ph), 4.99 [t, <i>J</i> (HP) 12.1, PCH ₂ P]	202.34 (s, br, 15CO at 293 K)	−121.04 (s, br at 293 K), −120.76 [2 d, <i>J</i> (PP) 34 at 190 K], −115.25 [2 d, <i>J</i> (PP) 34 at 190 K]	1430
2	2072s, 2035s, 2020vs, 1980m (sh), 1955w (sh), 1826w (br)	7.4 (m Ph), 2.45 [m, P(CH ₂) ₂ P]	202.93 (s, br, 15CO at 293 K)	−101.37 (s, br at 293 and 180 K)	1444
3	2071s, 2032s, 2020vs, 2001m (sh), 1990m (sh), 1960w (sh), 1831w (br)	7.4 (m Ph), 2.70 [dt, <i>J</i> (HP) 6.6, 10.2 PCH ₂ - CH ₂ CH ₂ P], 1.71 [dtt, <i>J</i> (HP) 12.2, 25.3, 30.1 PCH ₂ CH ₂ CH ₂ P]	203.42 (s, br, 15CO at 293 K)	−91.96 (s, br at 293 K), −90.53 [2 d, <i>J</i> (PP) 43.2 at 192 K], −86.80 [2 d, <i>J</i> (PP) 43.2 at 192 K]	1458
4a	2084m, 2056s, 2045s (sh), 2031vs, 1983w, 1832vw (br)	7.43 (m Ph), 2.62 [m, br, PCH ₂ (CH ₂) ₂ - CH ₂ P], 1.44 [m, br, PCH ₂ CH ₂ CH ₂ CH ₂ P]		−104.01 [d, ³ <i>J</i> (PP) 35.9 at 293 K], −157.22 [d, ³ <i>J</i> (PP) 35.9 at 293 K]	1500
4b	2070m, 2031s, 2020vs, 2001m (sh), 1976w, 1948w (sh), 1826vw (br)	7.4 (m Ph), 2.6 [m, PCH ₂ (CH ₂) ₂ CH ₂ P], 1.62 [m, PCH ₂ CH ₂ CH ₂ CH ₂ P]		−84.83 (s, at 293 K), −83.77 [2 d, <i>J</i> (PP) 49.1 at 187 K], −79.20 [2 d, <i>J</i> (PP) 49.1 at 187 K]	1472

^a Measured in CH₂Cl₂. ^b Chemical shifts (δ) in ppm and coupling constants in Hz; measured in CD₂Cl₂. ^c Using ¹⁰²Ru.

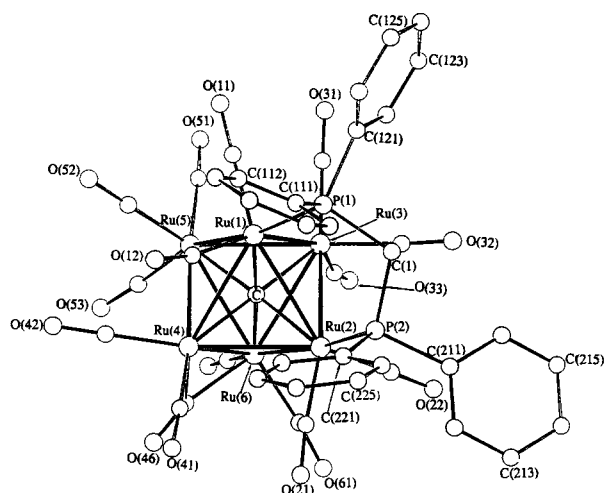


Fig. 1 Molecular structure of the hexanuclear cluster [Ru₆C(CO)₁₅-(μ-Ph₂PCH₂PPh₂)] **1** showing the crystallographic numbering scheme. The carbon atom of each carbonyl group has the same numbering as that of the oxygen atom

standing in CH₂Cl₂ for longer than 48 h decomposition occurred to yield at least nine other unidentified products; consequently manipulations were carried out under an argon atmosphere. The ¹H NMR spectrum of **4b** shows multiplets at δ 2.60 and 1.62 (Table 1). The ³¹P-¹H NMR spectrum shows a single peak for the two equivalent phosphorus atoms of the dppb ligand at 293 K which resolves into two signals for inequivalent P atoms on cooling to 187 K. There is no evidence for any isomers of the diphosphine-bridged compounds **1–3** or **4a** which is in contrast to the results obtained for Os₃-, Os₅- and Ru₅-based systems where incorporation of diphosphine ligands leads to isomers which differ in the mode of bonding of the phosphine.^{7–9,15,16}

The structures of the hexanuclear clusters [Ru₆C(CO)₁₅{μ-Ph₂P(CH₂)_nPPh₂}] (*n* = 1 **1**, 2 **2** or 3 **3**) have been determined by single-crystal X-ray diffraction studies and are displayed in Figs. 1–3 respectively; selected bond distances and angles are in Table 2. The structures are represented in a comparable manner to emphasise the similarity between them. Thus the corresponding Ru–P–P–Ru dihedral values in all the clusters show positive values, increasing from 13.5 in **1** to 24.3 in **2** and to 51.86° in

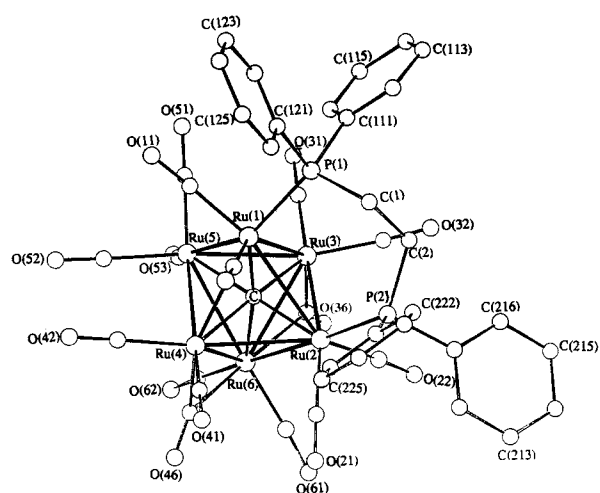


Fig. 2 Molecular structure of the hexanuclear cluster [Ru₆C(CO)₁₅-(μ-Ph₂P(CH₂)₂PPh₂)] **2**. Details as in Fig. 1

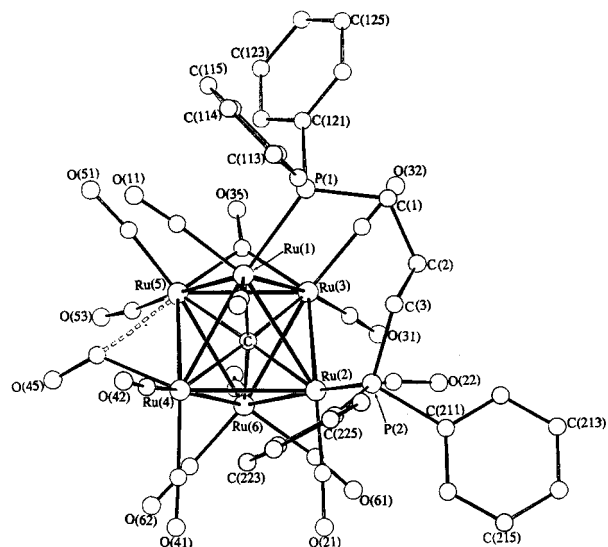


Fig. 3 Molecular structure of the hexanuclear cluster [Ru₆C(CO)₁₅-(μ-Ph₂P(CH₂)₃PPh₂)] **3**. Details as in Fig. 1

Table 2 Selected comparative bond distances (Å) and angles (°) for $[\text{Ru}_6\text{C}(\text{CO})_{15}\{\mu\text{-Ph}_2\text{P}(\text{CH}_2)_n\text{PPh}_2\}]$ ($n = 1, 2, 3$)

	1	2	3		1	2	3
Ru(1)–Ru(2)	2.989(1)	3.029(1)	2.998(3)	Ru(3)–C(31)	1.895(13)	1.876(9)	1.86(3)
Ru(1)–Ru(3)	2.902(1)	3.138(1)	3.020(3)	Ru(3)–C(32)	1.876(14)	1.894(9)	1.86(3)
Ru(1)–Ru(4)	2.977(1)	2.864(1)	2.909(4)	Ru(3)–C(33)	1.929(14)	—	—
Ru(1)–Ru(5)	2.878(1)	2.868(1)	2.942(3)	Ru(4)–C(41)	1.899(14)	1.882(10)	1.90(5)
Ru(2)–Ru(3)	2.904(1)	2.861(1)	2.965(3)	Ru(4)–C(42)	1.878(13)	1.884(9)	1.82(4)
Ru(2)–Ru(4)	2.941(1)	2.956(1)	2.947(3)	Ru(5)–C(51)	1.929(14)	1.886(11)	1.75(4)
Ru(2)–Ru(6)	2.871(1)	2.877(1)	2.893(3)	Ru(5)–C(52)	1.906(14)	1.922(11)	1.82(3)
Ru(3)–Ru(5)	2.906(1)	2.826(1)	2.830(3)	Ru(5)–C(53)	1.899(13)	1.879(11)	—
Ru(3)–Ru(6)	2.942(1)	2.877(1)	2.838(3)	Ru(6)–C(61)	1.873(16)	1.890(10)	1.91(3)
Ru(4)–Ru(5)	2.862(1)	2.979(1)	2.907(4)	Ru(6)–C(62)	1.875(14)	1.903(10)	1.79(4)
Ru(4)–Ru(6)	2.844(1)	2.815(1)	2.877(4)	Ru(6)–C(63)	—	—	1.83(4)
Ru(5)–Ru(6)	2.901(1)	2.919(1)	2.869(4)	Ru(4)–C(46)	2.065(13)	2.001(8)	—
Ru(1)–C	2.049(11)	2.039(7)	2.07(3)	Ru(6)–C(46)	2.077(12)	2.193(8)	—
Ru(2)–C	2.029(11)	2.023(7)	2.01(3)	Ru(3)–C(36)	—	1.994(9)	—
Ru(3)–C	2.041(11)	2.042(7)	2.04(3)	Ru(6)–C(36)	—	2.284(9)	—
Ru(4)–C	2.077(11)	2.085(7)	2.07(3)	Ru(3)–C(35)	—	—	1.97(3)
Ru(5)–C	2.068(11)	2.081(7)	2.13(3)	Ru(5)–C(35)	—	—	2.04(3)
Ru(6)–C	2.087(11)	2.122(7)	2.07(3)	Ru(4)–C(45)	—	—	2.03(7)
Ru(1)–P(1)	2.347(3)	2.338(2)	2.384(8)	Ru(5)–C(45)	—	—	2.63(6)
Ru(2)–P(2)	2.333(3)	2.347(2)	2.346(7)	P(1)–C(1)	1.838(11)	1.830(8)	1.818(23)
Ru(1)–C(11)	1.878(16)	1.863(11)	1.86(3)	P(2)–C(1)	1.830(11)	—	—
Ru(1)–C(12)	1.895(15)	1.870(10)	1.85(3)	P(2)–C(2)	—	1.837(8)	—
Ru(2)–C(21)	1.862(14)	1.883(9)	1.81(4)	P(2)–C(3)	—	—	1.838(25)
Ru(2)–C(22)	1.896(12)	1.868(9)	1.90(3)				
Ru(3)–Ru(1)–Ru(2)	59.0(1)	55.3(1)	59.0(1)	Ru(6)–Ru(5)–Ru(3)	60.9(1)	60.1(1)	59.7(1)
Ru(4)–Ru(1)–Ru(2)	59.1(1)	60.1(1)	59.8(1)	Ru(6)–Ru(5)–Ru(4)	59.1(1)	57.0(1)	59.7(1)
Ru(4)–Ru(1)–Ru(3)	88.8(1)	86.4(1)	87.4(1)	Ru(3)–Ru(6)–Ru(2)	59.9(1)	59.6(1)	62.3(1)
Ru(5)–Ru(1)–Ru(2)	88.5(1)	88.0(1)	88.3(1)	Ru(4)–Ru(6)–Ru(2)	61.9(1)	62.6(1)	61.4(1)
Ru(5)–Ru(1)–Ru(3)	60.4(1)	55.9(1)	56.7(1)	Ru(4)–Ru(6)–Ru(3)	90.7(1)	92.6(1)	91.6(1)
Ru(5)–Ru(1)–Ru(4)	58.5(1)	62.6(1)	59.6(1)	Ru(5)–Ru(6)–Ru(2)	90.4(1)	90.0(1)	91.8(1)
Ru(3)–Ru(2)–Ru(1)	59.0(1)	64.3(1)	60.9(1)	Ru(5)–Ru(6)–Ru(3)	59.6(1)	58.4(1)	59.5(1)
Ru(4)–Ru(2)–Ru(1)	60.3(1)	57.2(1)	58.6(1)	Ru(5)–Ru(6)–Ru(4)	59.8(1)	62.6(1)	60.8(1)
Ru(4)–Ru(2)–Ru(3)	89.5(1)	90.0(1)	87.8(1)	Ru(2)–C–Ru(1)	94.3(5)	96.4(3)	95(1)
Ru(6)–Ru(2)–Ru(1)	89.7(1)	89.2(1)	89.1(1)	Ru(3)–C–Ru(1)	90.4(4)	100.5(3)	95(1)
Ru(6)–Ru(2)–Ru(3)	61.3(1)	60.2(1)	58.0(1)	Ru(3)–C–Ru(2)	91.0(4)	89.5(3)	94(1)
Ru(6)–Ru(2)–Ru(4)	58.6(1)	57.7(1)	59.0(1)	Ru(4)–C–Ru(1)	92.4(4)	88.0(3)	89(1)
Ru(2)–Ru(3)–Ru(1)	62.0(1)	60.4(1)	60.1(1)	Ru(4)–C–Ru(2)	91.5(4)	92.0(3)	92(1)
Ru(5)–Ru(3)–Ru(1)	59.4(1)	57.2(1)	60.3(1)	Ru(4)–C–Ru(3)	176.1(6)	171.2(4)	172(1)
Ru(5)–Ru(3)–Ru(2)	89.7(1)	92.2(1)	91.1(1)	Ru(5)–C–Ru(1)	88.7(4)	88.2(3)	89(1)
Ru(6)–Ru(3)–Ru(1)	90.0(1)	87.1(1)	89.7(1)	Ru(5)–C–Ru(2)	176.9(6)	174.4(4)	176(1)
Ru(6)–Ru(3)–Ru(2)	58.8(1)	60.2(1)	59.7(1)	Ru(5)–C–Ru(3)	90.0(4)	86.5(3)	86(1)
Ru(6)–Ru(3)–Ru(5)	59.5(1)	61.6(1)	60.8(1)	Ru(5)–C–Ru(4)	87.3(4)	91.3(3)	88(1)
Ru(2)–Ru(4)–Ru(1)	60.7(1)	62.7(1)	61.6(1)	Ru(6)–C–Ru(1)	176.9(6)	171.0(4)	175(1)
Ru(5)–Ru(4)–Ru(1)	59.0(1)	58.7(1)	60.8(1)	Ru(6)–C–Ru(2)	88.5(4)	87.9(3)	90(1)
Ru(5)–Ru(4)–Ru(2)	89.8(1)	87.3(1)	90.0(1)	Ru(6)–C–Ru(3)	90.9(4)	87.4(3)	87(1)
Ru(6)–Ru(4)–Ru(1)	90.5(1)	93.8(1)	91.2(1)	Ru(6)–C–Ru(4)	86.2(4)	84.0(3)	88(1)
Ru(6)–Ru(4)–Ru(2)	59.5(1)	59.7(1)	59.5(1)	Ru(6)–C–Ru(5)	88.6(4)	88.0(3)	86(1)
Ru(6)–Ru(4)–Ru(5)	61.1(1)	60.4(1)	59.5(1)	C(1)–P(1)–Ru(1)	111.5(4)	114.6(3)	119.9(8)
Ru(3)–Ru(5)–Ru(1)	60.2(1)	66.9(1)	63.1(1)	C(1)–P(2)–Ru(2)	114.4(4)	—	—
Ru(4)–Ru(5)–Ru(1)	62.5(1)	58.6(1)	59.6(1)	C(2)–P(2)–Ru(2)	—	118.8(3)	—
Ru(4)–Ru(5)–Ru(3)	91.0(1)	90.2(1)	91.2(1)	C(3)–P(2)–Ru(2)	—	—	115.0(8)
Ru(6)–Ru(5)–Ru(1)	91.4(1)	91.6(1)	90.7(1)				

3. The three clusters differ mainly in the nature of the bidentate ligand. The fundamental carbido-octahedral core of the parent compound $[\text{Ru}_6\text{C}(\text{CO})_{17}]^{17}$ is retained in all cases and the diphosphine ligand replaces two of the terminal carbonyl groups, spanning the Ru(1)–Ru(2) bond. Subtle variations in the degree of carbonyl bridging are evident between the three structures; **1** has one bridging carbonyl [Ru(4)–C(46) 2.065(13), Ru(6)–C(46) 2.077(12) Å], while **2** has one symmetrically bridging and one slightly asymmetric carbonyl ligand [Ru(4)–C(46) 2.001(8), Ru(6)–C(46) 2.193(8) Å] and **3** has one bridging and one semibridging carbonyl [Ru(3)–C(35) 1.97(3), Ru(5)–C(35) 2.04(3) and Ru(4)–C(45) 2.03(7), Ru(5)–C(45) 2.63(6) Å].

The Ru–Ru bond distances for all three cluster products are similar, and typical of those reported for related carbido-ruthenium clusters.¹⁸ The longest Ru–Ru bond in the diphosphine cluster **1** is that bridged by the dpmm ligand [Ru(1)–Ru(2) 2.989(1) Å], whereas in both the longer-chain analogues **2** and **3** the longest Ru–Ru bond is adjacent to the metal bond bridged by the diphosphine ligand [Ru(1)–Ru(3) 3.138(1) **2** and

Ru(1)–Ru(3) 3.020(3) Å **3**]. This unusual pattern is not readily explained but must be related to the change in the length of the organic backbone linking the two phosphorus atoms in the respective diphosphine ligands. The shortest Ru–Ru bond in all three structures is a μ -carbonyl-bridged bond [Ru(4)–Ru(6) 2.844(1) **1** Ru(4)–Ru(6) 2.815(1) **2**, Ru(3)–Ru(5) 2.830(3) **3**], whereas in the parent cluster $[\text{Ru}_6\text{C}(\text{CO})_{17}]^{13}$ the μ -CO-bridged bond is in the middle of the Ru–Ru range.¹⁷ The metal–carbide distances for all three compounds are equal, within experimental error, and within the range observed for related structures.¹⁸ It was anticipated that with the increase in the length of the methylene backbone in the diphosphine ligand in clusters **1**–**3** a greater degree of freedom would be available for the ligand to adopt a sterically favourable edge-bridging configuration on the metal surface. However, X-ray data show the opposite trend. Within experimental error, the mean Ru–P distances in all three clusters of the series are similar [2.340(3) **1**, 2.343(2) **2** and 2.365(8) Å **3**]. However, evidence of strain within the Ru–P–C ring system, arising from increasing the chain length in

Table 3 Crystallographic data and structure parameters for $[\text{Ru}_6\text{C}(\text{CO})_{15}\{\mu\text{-Ph}_2\text{P}(\text{CH}_2)_n\text{PPh}_2\}]$ ($n = 1$ **1**, 2 **2** and 3 **3**)^{*}

	1	2	3
Molecular formula	$\text{C}_{40}\text{H}_{22}\text{O}_{15}\text{P}_2\text{Ru}_6$	$\text{C}_{41}\text{H}_{24}\text{O}_{15}\text{P}_2\text{Ru}_6$	$\text{C}_{42}\text{H}_{26}\text{O}_{15}\text{P}_2\text{Ru}_6$
<i>M</i>	1423.16	1437.19	1451.22
Crystal dimensions/mm	$0.26 \times 0.24 \times 0.13$	$0.29 \times 0.22 \times 0.26$	$0.22 \times 0.20 \times 0.15$
Crystal system	Monoclinic	Monoclinic	Orthorhombic
Space group	<i>C2/c</i>	<i>I2/c</i>	<i>Pbca</i>
<i>a</i> /Å	14.122(3)	21.780(3)	24.769(3)
<i>b</i> /Å	18.147(3)	19.450(3)	18.054(3)
<i>c</i> /Å	35.687(5)	21.881(3)	21.114(3)
β /°	100.99(2)	93.26(2)	
<i>U</i> /Å ³	8977.85	9254.25	9441.75
<i>D_c</i> /g cm ⁻³	2.106	2.063	2.042
<i>F</i> (000)	5456	5520	5584
μ (Mo-K α)/mm ⁻¹	1.94	1.88	1.85
Number of reflections collected	4492	5344	3823
Number of independent reflections merged	4071	5006	2369
Number of reflections used for refinement [$I > 3\sigma(I)$]	3918	5001	2346
Step width/°	0.70	0.80	0.70
Number of refined parameters	399	403	265
Converged residual <i>R</i>	0.0397	0.0373	0.0638
$R' [= \sum(F_o - F_c) / \sum F_o]$	0.0410	0.0378	0.0622
$\rho_{\text{max}}, \rho_{\text{min}}/e \text{ \AA}^{-3}$	0.30, -0.48	0.60, -0.57	0.70, -0.46

^{*} Details in common: cell determined from 25 reflections in the range 2θ 15–25°; $Z = 8$; 298 K; 2θ scan range 3.0–50.0°; scan mode ω -2 θ ; <5% variation in intensity.

the diphosphine ligand, in clusters **1–3** is detectable when the Ru–P–C angles are compared. The mean Ru–P–C intercylic angle in the dppm cluster **1** is near tetrahedral [112.5(3)°] whereas in the dppe and dppp analogues this angle becomes distorted to larger values [116.7(4)° in **2** and 117.5(8)° in **3**]. The substitution pattern observed for this series of compounds appears to be dependent on the length of the organic chain linking the two phosphorus atoms in the diphosphine ligands used. Although an edge-bridging bonding mode is adopted in most of the clusters reported, the increase in chain length appears to induce considerable conformational strain within the ligand and would explain why the reaction with the dppb ligand generates, as the major product, a compound in which the diphosphine ligand adopts the more unusual pendant coordination mode.

Experimental

All reactions were carried out under nitrogen using dry degassed solvents. Infrared spectra were recorded on a Perkin-Elmer 983 spectrophotometer, NMR (¹H, ¹³C and ³¹P-¹H) spectra on Bruker WM 250 and WH 400 instruments using CD₂Cl₂ and P(OMe)₃ as internal references respectively and electron-impact mass spectra on a NEI MS 12 spectrometer using tris(perfluoroheptyl)-*s*-triazine as calibrant. Microanalyses were performed in the University Chemical Laboratory, Cambridge. The diphosphines, dppm, dppe, dppp and dppb, were obtained from Strem Chemicals and the parent cluster [Ru₆C(CO)₁₇] was prepared by the literature method.¹⁹

Preparations

[Ru₆C(CO)₁₅{μ-Ph₂PCH₂PPh₂}] 1. The complex [Ru₆C(CO)₁₇] (75 mg, 0.0686 mmol) was suspended in hexane (15 cm³) and dppm (28 mg, 0.0703 mmol) added to the refluxing solution. The reaction mixture was monitored by IR spectroscopy; a change from red to pale orange occurred after 30 min together with precipitation of the product [Ru₆C(CO)₁₅{μ-Ph₂PCH₂PPh₂}] **1**. The mixture was then filtered through a sintered funnel and the red solid **1** washed with cold hexane (3 × 10 cm³ portions). Black crystals were obtained by slow diffusion of a layered CH₂Cl₂–hexane solution under N₂ over 24 h (yield 92 mg, 94%) (Found: C, 33.85; H, 1.45; P, 4.4. Calc. for C₄₀H₂₂O₁₅P₂Ru₆: C, 33.6; H, 1.55; P, 4.35%).

[Ru₆C(CO)₁₅{μ-Ph₂P(CH₂)₂PPh₂}] 2. The complex [Ru₆C(CO)₁₇] (75 mg, 0.0686 mmol) was suspended in hexane (15 cm³) and dppe (28 mg, 0.0704 mmol) added to the refluxing solution. The reaction mixture was monitored by IR spectroscopy; a change from red to pale orange occurred after 30 min together with precipitation of the product [Ru₆C(CO)₁₅{μ-Ph₂P(CH₂)₂PPh₂}] **2**. The reaction mixture was then filtered through a sintered funnel and red solid **2** was washed with cold hexane (3 × 10 cm³ portions). Black crystals were obtained by slow diffusion of a layered CH₂Cl₂–hexane solution under N₂ over 24 h (yield 88 mg, 90%) (Found: C, 34.5; H, 1.9; P, 4.35. Calc. for C₄₁H₂₄O₁₅P₂Ru₆: C, 34.2; H, 1.65; P, 4.3%).

[Ru₆C(CO)₁₅{μ-Ph₂P(CH₂)₃PPh₂}] 3. The complex [Ru₆C(CO)₁₇] (75 mg, 0.0686 mmol) was suspended in hexane (15 cm³) and dppp (28 mg, 0.0705 mmol) added to the refluxing solution. The reaction mixture was monitored by IR spectroscopy; a change from red to pale orange occurred after 30 min together with precipitation of the product [Ru₆C(CO)₁₅{μ-Ph₂P(CH₂)₃PPh₂}] **3**. The reaction mixture was then filtered through a sintered funnel and red solid **3** was washed with cold hexane (3 × 10 cm³ portions). Black crystals were obtained by slow diffusion of a layered CH₂Cl₂–hexane solution under N₂ over 24 h (yield 85 mg, 87%) (Found: C, 34.95; H, 1.85; P, 4.6. Calc. for C₄₂H₂₆O₁₅P₂Ru₆: C, 34.7; H, 1.8; P, 4.25%).

[Ru₆C(CO)₁₆{Ph₂P(CH₂)₄PPh₂-P}] 4a and [Ru₆C(CO)₁₅{μ-Ph₂P(CH₂)₄PPh₂}] 4b. The complex [Ru₆C(CO)₁₇] (75 mg, 0.0686 mmol) was suspended in hexane (15 cm³) and dppb (29 mg, 0.0705 mmol) added to the refluxing solution. The reaction mixture was monitored by IR spectroscopy and was complete after 30 min with a change from red to pale orange and precipitation of the product [Ru₆C(CO)₁₆{Ph₂P(CH₂)₄PPh₂-P}] **4a**. The mixture was then reduced in volume on a rotary evaporator and eluted with 30% dichloromethane–70% hexane to yield **4a** as the major product at *R_f* 0.4, followed by a brown band of [Ru₆C(CO)₁₅{μ-PPh₂(CH₂)₄PPh₂}] **4b** at *R_f* 0.55. Black crystals of **4a** were obtained by slow diffusion of a layered CH₂Cl₂–hexane solution under N₂ over 24 h, (yield 72 mg, 74%) (Found: C, 35.45; H, 2.0; P, 4.35. Calc. for C₄₄H₂₈O₁₆P₂Ru₆: C, 35.2; H, 1.9; P, 4.25%). A black crystalline powder of **4b** was obtained by slow diffusion of a layered CH₂Cl₂–hexane solution under N₂ over 72 h (Found: C, 35.4; H, 2.05; P, 4.4. Calc. for C₄₃H₂₈O₁₅P₂Ru₆: C, 35.25; H, 1.9; P, 4.2%).

Crystallography

Suitable crystals of compounds **1–3** were grown from slow diffusion of a layered CH₂Cl₂–hexane solution under nitrogen over 24 h at room temperature. Those of **3** were relatively poor in quality compared to those for **1** and **2**. Several attempts to recrystallise compound **3** to yield crystals of better quality failed. Additionally, a low-temperature study for this compound could not be carried out on the Philips PW 1100 diffractometer. Details of crystal parameters, data-collection parameters, and refinement data are summarised in Table 3. The method of data collection and processing used has been described previously.²⁰ For all three clusters the positions of the metal atoms were deduced from a Patterson synthesis and the remaining non-hydrogen atoms were located from subsequent Fourier-difference syntheses.²¹ Empirical absorption corrections were applied to each data set after initial refinement of the isotropic parameters of all the non-hydrogen atoms.²² During the final cycles of refinement of structures **1** and **2** anisotropic thermal parameters were assigned to the six metal, two phosphorus and carbido atoms together with the atoms of the carbonyl ligands. For structure **3**, anisotropic thermal parameters were assigned to only the six metal and two phosphorus atoms. The six carbon atoms of each phenyl ring of the respective bidentate phosphine groups in **1–3** were grouped as rigid hexagons ($dC-C$ 1.395 Å, $C-C-C$ 120°) with the phenyl H atoms geometrically calculated to ride at the respective carbon atoms ($C-H$ 1.08 Å), with fixed thermal parameters of 0.08 Å². The hydrogen atoms of the methylene carbon atoms on the backbone of each diphosphine ligand were also geometrically calculated to ride at the respective carbon atoms at distances of 1.08 Å with fixed thermal parameters of 0.08 Å².

Full-matrix refinement (on F) of the atomic positional and thermal parameters of all the non-hydrogen atoms in the structures **1–3** converged at final R and R' values of 0.0397 and 0.0410 for **1**, 0.0373 and 0.0378 for **2** and 0.0638 and 0.0622 for **3**, respectively with weights of $w = 1/\sigma^2(F_o)$ assigned to individual reflections.

Atomic coordinates, thermal parameters, and bond lengths and angles have been deposited at the Cambridge Crystallographic Data Centre (CCDC). See Instructions for Authors, *J. Chem. Soc., Dalton Trans.*, 1997, Issue 1. Any request to the CCDC for this material should quote the full literature citation and the reference number 186/354.

Acknowledgements

We would like to thank the SERC for financial support and for

access to the Chemical Database Service at Daresbury and to St. John's College Cambridge for the award of a Research fellowship (to S. R. D.).

References

- 1 H. A. Mayer and W. C. Kaska, *Chem. Rev.*, 1994, **94**, 1239.
- 2 R. Puddephatt, *Chem. Soc. Rev.*, 1983, **12**, 99.
- 3 M. P. Brown, J. R. Fisher, R. H. Hill, R. J. Puddephatt and K. R. Seddon, *Inorg. Chem.*, 1981, **20**, 3516.
- 4 M. P. Brown, P. A. Dolby, M. M. Harding, A. J. Mathews and A. K. Smith, *J. Chem. Soc., Dalton Trans.*, 1993, 1671.
- 5 T. Adatia, S. S. D. Brown and I. D. Salter, *J. Chem. Soc., Dalton Trans.*, 1993, 559.
- 6 D. Braga, U. Matteoli, P. Sabatino and A. Scrivanti, *J. Chem. Soc., Dalton Trans.*, 1995, 419.
- 7 B. F. G. Johnson, J. Lewis, P. R. Raithby, M. J. Rosales and D. A. Welsh, *J. Chem. Soc., Dalton Trans.*, 1986, 453.
- 8 M. I. Bruce, T. W. Hambley, B. K. Nicholson and M. R. Snow, *J. Organomet. Chem.*, 1982, **235**, 83.
- 9 J. Evans, B. P. Gracey, L. R. Gray and M. Webster, *J. Organomet. Chem.*, 1982, **240**, C61.
- 10 B. F. G. Johnson, J. Lewis, J. N. Nicholls, J. Puga, P. R. Raithby, M. J. Rosales, M. McPartlin and W. Clegg, *J. Chem. Soc., Dalton Trans.*, 1983, 277.
- 11 S. C. Brown, J. Evans and M. Webster, *J. Chem. Soc., Dalton Trans.*, 1981, 2263.
- 12 T. Blum, M. P. Brown, B. T. Heaton, A. S. Hor, J. A. Iggo, J. S. Z. Sabounchei and A. K. Smith, *J. Chem. Soc., Dalton Trans.*, 1994, 513.
- 13 J. Evans, B. P. Gracey, L. R. Gray, A. G. Jones and M. Webster, *Acta Crystallogr., Sect. C*, 1987, **43**, 2286.
- 14 B. E. Mann, *J. Chem. Soc., Dalton Trans.*, 1973, 2012.
- 15 B. E. Hanson, P. E. Fanwick and J. S. Mancini, *Inorg. Chem.*, 1982, **21**, 3811.
- 16 A. J. Deeming, S. Donovan-Mtunzi and S. E. Kabir, *J. Organomet. Chem.*, 1987, **333**, 253.
- 17 A. Sirigu, M. Bianchi and E. Benedetti, *Chem. Commun.*, 1969, 596; D. Braga, F. Grepioni, P. J. Dyson, B. F. G. Johnson, P. Frediani, M. Bianchi and F. Piacenti, *J. Chem. Soc., Dalton Trans.*, 1992, 2565.
- 18 D. Braga, P. J. Dyson, F. Grepioni and B. F. G. Johnson, *Chem. Soc. Rev.*, 1994, **94**, 1585.
- 19 B. F. G. Johnson, J. Lewis, S. W. Sankey, K. Wong, M. McPartlin and W. J. H. Nelson, *J. Organomet. Chem.*, 1980, **191**, C3.
- 20 P. F. Jackson, B. F. J. Johnson, J. Lewis, W. J. H. Nelson and M. McPartlin, *J. Chem. Soc., Dalton Trans.*, 1982, 2099.
- 21 G. M. Sheldrick, SHELX 76, Program for Crystal Structure Determination, University of Cambridge, 1976.
- 22 N. Walker and D. Stuart, *Acta Crystallogr., Sect. A*, 1983, **39**, 158.

Received 2nd September 1996; Paper 6/06040D